Suppression of Undesired Attractors in a Self-Oscillating H-Bridge Parallel Resonant Converters Under Zero Current Switching Control

A. El Aroudi, *Senior Member, IEEE*, L. Benadero, E. Ponce, C. Olalla, *Member, IEEE*, F. Torres, L. Martinez-Salamero, *Senior Member, IEEE*

Abstract—Resonant converters under zero current switching control strategy can exhibit coexistence of attractors, making it difficult the startup of the system from zero initial conditions. In this paper, the problem of multiple coexisting attractors in parallel resonant converters is addressed. Appropriate modifications of the switching decision with the aim of converting undesired attractors into virtual ones are proposed. A suitable control signal is generated from the state variables of the system and used to adjust the switching decision. Numerical simulations corroborate the proposed solutions and the simplest one was finally verified by measurements from a laboratory prototype.

I. INTRODUCTION

RESONANT converters are used in many industrial applications to meet the high efficiency and power density requirements [1], [2]. Dynamic behavior and steady-state analysis of these systems have attracted and are still attracting the interest of many researchers [3]–[6]. Most of the existing works assume that the quality factor is sufficiently high and that the switching frequency coincides with the resonant frequency such that the system waveforms can be considered sinusoidal. Hence, a simplified frequency-domain ac analysis based on the first harmonic approach can be used [5], [6]. Under low quality factor conditions, significant errors appear, so disqualifying the previous approach [7].

Moreover, like other switched systems, power converters are nonsmooth dynamical systems prone to exhibit peculiar phenomena such as border collision bifurcations and coexistence of attractors [8], [9]. This is a serious problem for designers of these systems since the coexistence of undesired basin of

A. El Aroudi, C. Olalla and L. Martinez-Salamero are with Universitat Rovira i Virgili, Departament d'Enginyeria Electrònica, Elèctrica i Automàtica, Escola Tècnica Superior d'Enginyeria, 43007, Tarragona, Spain (e-mail:abdelali.elaroudi@urv.cat).

L. Benadero is with Universitat Politècnica de Catalunya (UPC), Departament de Física, Barcelona, Spain.

E. Ponce and F. Torres are with Universidad de Sevilla, Instituto de Matemáticas (IMUS), Universidad de Sevilla (US), Sevilla, Spain.

attractions can make difficult the startup of the system with zero initial conditions (ICs).

In [10]–[12], nonlinear nonsmooth bifurcation phenomena and the occurrence of coexistence of attractors have been theoretically explored by using the switched two-dimensional piecewise linear continuous-time model of a dc-ac Parallel Resonant Converter (PRC) under Zero Current Switching (ZCS) control. There, it was shown by performing bifurcation analysis of a nonsmooth model, that the system can exhibit up to three basins of attraction. It was also shown that for relatively low values of quality factors, the system cannot startup with zero initial conditions under the conventional ZCS control. In a practical power electronic converter, coexistence of attractors is undesired and it is necessary to avoid it. A first attempt to suppress this phenomenon in a PRC was done in [10], where it was shown that by appropriately modifying the switching decision of the system, the problem of startup with zero initial conditions can be solved. In this brief, the technique proposed in [10] is further explored and two other control schemes are proposed showing their effectiveness to suppress the undesired basin of attractions. An experimental validation of the most simple solution from the three proposed strategies is also provided.

The rest of the paper is organized as follows. In Section II, the state space of the LC PRC is described providing its different possible steady-state solutions. Then, the proposed solutions for avoiding undesired coexisting attractors are described in Section III. Numerical simulations and their experimental validation are given in Sections IV and V. The conclusions are reported in Section VI.

II. THE LC PRC CONVERTER UNDER ZCS CONTROL

A. System description

Figure 1 shows the equivalent circuit diagram of the system considered in this study, which consists in a PRC under ZCS control [3], [4]. Roughly speaking, the PRC is a switched system that includes a resonant tank circuit and a switching network that actively select the input voltage applied to the tank. Namely, $v_s = V_g$ when $i_L > 0$ and $v_s = -V_g$ when $i_L < 0$. The circuit operation is based on an automatically activated switching between two configurations, each of them leading to a particular circuit topology, which can be described by a linear dynamical model. It is clear that if no switching is performed, the capacitor voltage and the inductor current will

Fig. 1. Block diagram of the LC PRC under ZCS control.

Fig. 2. State plane showing different switching manifolds obtained by modifying the ZCS thresholds. An illustrative limit cycle is also shown.

tend to constant values corresponding to equilibrium points of the two linear topologies, with positive values if $u = 1$ ($\delta = 1$ and $\bar{\delta} = 0$), and its symmetrical values if $u = -1$ ($\delta = 0$ and $\bar{\delta} = 1$)). The variable u is determined by the ZCS control strategy such that $u = 1$ if $i_L > 0$, and $u = -1$ if $i_L < 0$, i.e., $u = \text{sign}(i_L)$. Notice that for high values of the quality factor Q, this strategy always induce a stable limit cycle. However, depending on the starting conditions, the dynamics could be addressed to undesired equilibrium points. Based on an accurate mathematical analysis, it was shown in [11] that if Q is lower than a critical value $Q_{\text{hc}} \approx 2.6$, the normal zero initial condition lies on the basin of attraction of undesired equilibrium and so the desired steady-state limit cycle would not be reached. Note also that according to the ZCS control rule, we have two configurations and so we define the corresponding partitions in the state-plane: $\Sigma^+ = \{(v_C, i_L) : i_L > 0\}$ and $\Sigma^- = \{(v_C, i_L) : i_L < 0\}$. Performing a steady-state analysis for the equivalent linear circuits of Fig. 1 for $u = 1$ and $u = -1$, the respective equilibria are given by

$$\mathbf{x}_q^+ = \begin{pmatrix} V_q \\ I_q \end{pmatrix} = \begin{pmatrix} V_g \\ \dfrac{V_g}{R} \end{pmatrix}, \quad \mathbf{x}_q^- = -\begin{pmatrix} V_g \\ \dfrac{V_g}{R} \end{pmatrix}, \quad (1)$$

where R is the load resistance and V_g is the input voltage. Both equilibria are stable and located in their respective corresponding partitions that is $\mathbf{x}_q^+ \in \Sigma^+$ and $\mathbf{x}_q^- \in \Sigma^-$ so they are natural real equilibria and can be attracting for some initial conditions. This is undesired in practice because the normal operation of this converter is a limit cycle.

III. PROPOSALS FOR ACHIEVING GLOBAL CONVERGENCE TO THE DESIRED LIMIT CYCLE

The construction of the state-plane trajectories for the switched model of the system greatly facilitates the study of the global dynamics. The main reason for coexistence of attractors to take place in the PRC under ZCS control is that the stable equilibrium points $\mathbf{x}_q^-$ and $\mathbf{x}_q^+$ for each linear topology are also real attractors for the switched system, as mentioned before. Hence, to avoid coexistence of attractors and guarantee the startup of the system and its convergence to its desired crossing limit cycle from any initial condition, the switching decision must be changed in such a way that these equilibria become virtual. To fulfill this, the driving signal u can be generated according to the following expression
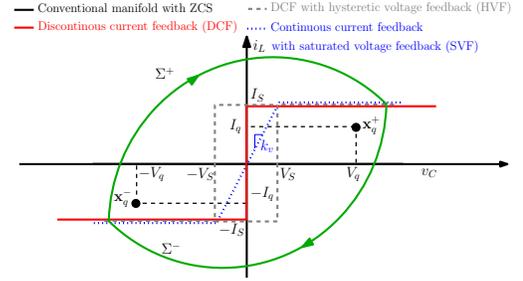
$$u = \text{sign}(i_L - i_S), \quad (2)$$

where i_S is a threshold signal generated either according to an extra voltage feedback loop or by introducing a hysteresis in the current loop as will be detailed later. Note that the conventional ZCS control can be recovered by making $i_S = 0$. Therefore, after some operating cycles, i_S can be switched to zero if the advantages of the ZCS control are to be maintained in steady-state operation. This is because once the trajectory enters the basin of attraction of the desired limit cycle, the conventional ZCS control strategy is enough to maintain the system in this limit cycle. Fig. 2 shows, in the state plane, the switching boundaries corresponding to different possible choices of the control signal i_S to make the undesired equilibria virtual and to achieve global convergence to the desired limit cycle. Namely, if $i_S = 0$, one has the conventional ZCS control which is represented in the mentioned state plane by the line whose equation is $i_L = 0$. Other control schemes together with their corresponding expressions of the threshold signal i_S are detailed below.

A. Discontinuous current feedback (DCF)

The first proposed technique to make the undesired equilibria virtual, which was presented in [10], is to choose the signal i_S according to the following expression

$$i_S = I_S \text{sign}(v_C). \quad (3)$$

where I_S is a suitable constant. To obtain this control scheme, the inductor current i_L is compared with two fixed symmetrical values, namely I_S for $v_C > 0$ and $-I_S$ for $v_C < 0$, by using two ad hoc comparators. In this way, I_S and $-I_S$ become the new threshold currents. During startup, the value of I_S must be larger than I_q for the equilibrium points to be virtual but smaller than the maximum overshoot I_p of the inductor current for allowing a crossing to occur with I_S or $-I_S$. The maximum overshoot I_p is given by

$$I_p = I_q \left(1 + e^{-\frac{\pi}{\sqrt{4Q^2 - 1}}} \right), \quad Q = R\sqrt{\frac{C}{L}}. \quad (4)$$

Note that no overshoot exists for $Q < 1/2$ and that oscillation cannot take place in this case. In fact, limit cycles only exist for quality factor values higher than $Q_{\text{sn}} \approx 1.9$ [10], [11].

B. DCF with additional hysteretic voltage feedback (HVF)

Unfortunately, the above proposed control modification on the conventional ZCS has an important unexpected drawback.

Namely, as will be shown later by numerical simulations, an undesired high frequency chattering takes place at the discontinuity of the switching boundary ($v_C = 0, |i_L| < I_S$) due to the creation of a new small unstable limit cycle centered at the origin which is converted to a locally stable equilibrium point for the switched system under the new control strategy. This makes the startup of the system with zero initial condition impossible even with high quality factor values. Only if started at an initial current such that $|i_L(0)| \geq I_S$, the system will converge to the desired limit cycle. Therefore, an extra modification in the switching decision is required to overcome this unexpected emerging problem. A possible solution is based on splitting the set ($v_C = 0, |i_L| < I_S$) in the previous scheme into two segments ($v_C = \pm V_S, |i_L| < I_S$) by hysteretic feedback in the voltage loop. Now, the voltage v_C is compared with a signal V_S and its opposite value $-V_S$ and the result of the comparison is used to decide if I_S or $-I_S$ is to be chosen for comparing i_L so the new expression in (2) for the control signal i_S becomes

$$i_S = I_S \text{sign}(v_C \pm V_S), \tag{5}$$

where the minus sign applies when $u = 1$ and the plus sign applies when $u = -1$. In this way, the chattering phenomenon close to the origin can be completely suppressed as will be shown later using numerical simulations.

C. Continuous current feedback with additional saturated voltage feedback (SVF)

The previous modification, although provides an effective solution to the problem of chattering phenomenon if started at the origin, it unfortunately adds complexity to the control circuitry. A simpler way to avoid coexistence of attractors and also the chattering phenomenon without adding complexity, is by using a continuous switching manifold which includes output voltage feedback with a static gain k_v when this voltage is within the interval $(-V_S, V_S)$. The feedback is saturated when the signal $k_v v_C$ provided by the same feedback reaches the extremes of this interval. The gain $k_v = I_S/V_S$ must be larger than I_q/V_q to make equilibria virtual and must be smaller than a critical value to avoid that the steady-state orbit to be trapped in the linear zone of the saturation function. Now, the inductor current i_L is compared with a signal i_S, which is provided by the output of the saturable voltage feedback and the resulting expression for the control signal i_S becomes

$$i_S = \begin{cases} -I_S, & \text{for } v_C < -V_S, \\ \dfrac{I_S}{V_S} v_C, & \text{for } -V_S < v_C < V_S, \\ I_S, & \text{for } v_C > V_S. \end{cases} \tag{6}$$

Note that this control scheme becomes equivalent to the DCF technique when $k_v \to \infty$.

D. Hysteretic current feedback and edge-triggered flip-flop

The chattering phenomenon in the first proposed switching decision can be avoided by introducing a simple hysteretic loop in the current feedback without using information about
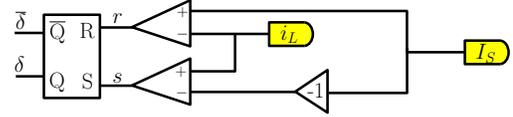

Fig. 3. Block diagram of the control strategy to avoid coexistence of attractors and chattering phenomena based on the hysteretic current feedback.
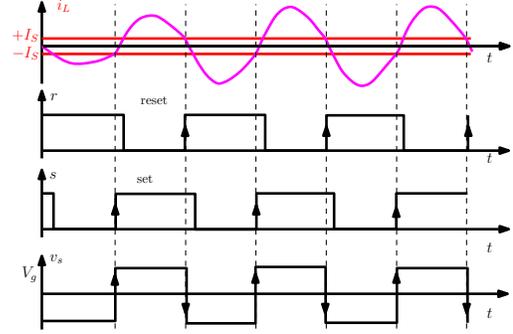

Fig. 4. Key waveforms corresponding to the control scheme described in Section IV-D.

the sign of the capacitor voltage, hence, avoiding extra complexity. In this case, the inductor current is compared with two symmetrical values $-I_S$ and I_S using two comparators and their respective outputs s and r are applied to a SR flip-flop which is edge-triggered as depicted in Fig. 3, according to which the signal i_S is generated and resulting in the key waveforms shown in Fig. 4.

This new control scheme has the advantages of all the previous techniques while avoiding chattering phenomenon and being its implementation simple.

IV. SIMULATION RESULTS

To illustrate the operation of the proposed control schemes, the parameters values: $V_g = 20$ V, $L = 7.3$ μH, $C = 10.7$ nF, $I_S = (I_p + I_q)/2 \approx 0.45$ A, are used. Let us select a value of load resistance $R = 54$ Ω for which coexistence of attractors is prominent. The corresponding value of the quality factor is
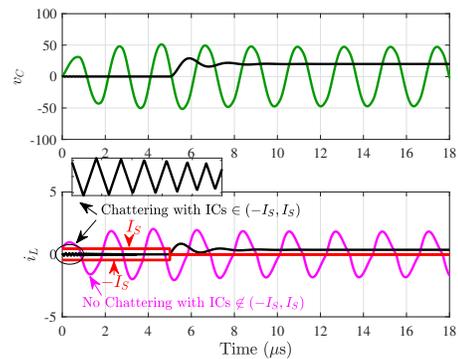

Fig. 5. Time-domain waveforms showing the behavior of the PRC with $R = 54$ Ω using the control signal defined in (3).Green and pink waveforms correspond to the orbit converging to the limit cycle, if ICs $\notin \{-I_S, I_S\}$. Otherwise, the chattering phenomenon takes place (see the black lines). The red lines stand for the defined boundary $I_S \approx 0.45$ A, if $t < 5$ μs.
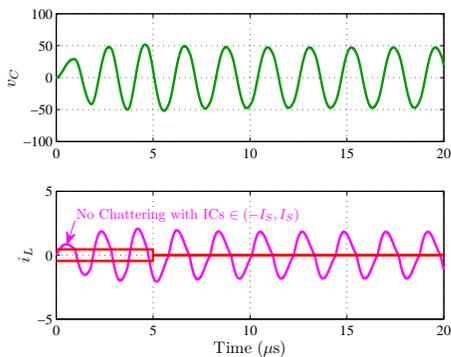
Fig. 6. Time-domain waveforms showing the behavior of the PRC with $R = 54\ \Omega$ using the DCF with additional HVF to avoid chattering phenomenon close to the origin. Note that this phenomenon does not take place even if ICs $\in \{-I_S, I_S\}$. $I_S \approx 0.45$ A and $V_S = 5$ V.
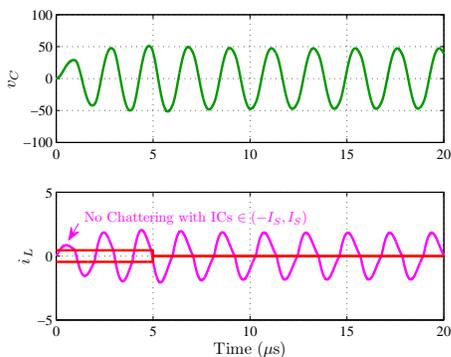

Fig. 7. Time-domain waveforms showing the behavior of the PRC with $R = 54\ \Omega$ using the SVF. $I_S \approx 0.45$ A and $V_S = 5$ V.

$Q \approx 2.1 < Q_{\text{hc}}$. For this value of quality factor, if the system is started at zero ICs using the conventional ZCS control, the trajectory will not converge to the desired limit cycle [10], [11]. In the simulations shown below, at $t = 5\ \mu$s, the modified control strategies are disabled and the system operates according to the conventional ZCS control strategy. Fig. 5 shows the time-domain waveforms of the state variables with the switching decision based on the discontinuous switching manifold starting from two different initial conditions. Because this modification only takes place during startup (5 μs in this case), the resulting limit cycle in steady-state is not altered. It can be observed that as stated before, with initial conditions outside the set $(v_C = 0, |i_L| < I_S)$, which includes the origin, the system reaches the stable crossing limit cycle in few switching periods. However, orbits starting at this set do not converge yet to the stable crossing limit cycle. Fig. 6 shows the time-domain waveforms of the state variables with the switching decision based on the discontinuous switching manifold with the additional hysteretic voltage feedback. As before, because the modification only takes place during 5 μs, the resulting limit cycle in steady-state is not altered. Note that with the extra modification, orbits even starting nearby the origin converge to the stable limit cycle. By means of this control scheme, undesired coexistence of attractors is fully

suppressed and the whole state-plane becomes the new basin of attraction of the desired limit cycle. Fig. 7 shows the time-domain waveforms of the state variables with the switching decision based on the switching manifold with saturable voltage feedback. Like in the previous case, orbits, even starting nearby the origin, converge to the stable limit cycle without any chattering phenomenon. Therefore, except for the case of (3), with all the proposed control schemes, the undesired coexistence of attractors can be fully suppressed and the whole state-plane becomes the new basin of attraction of the desired limit cycle with appropriate values of the control parameters I_S and V_S. In the next section, an experimental validation will be provided for the technique based on hysteretic current feedback and edge-triggered flip-flop.

V. EXPERIMENTAL VALIDATION

To validate the theoretical results and the numerical simulation, an experimental prototype of a H-bridge PRC has been built. The power stage consists of four MOSFETs (IPB200N15N3) activated by a circuit based on the driver UCC27210. The resonant capacitance corresponds to three parallel connected high-quality low-ESR NP0/CG0 capacitors (C=2×4.7 nF+1 nF). The resonant inductor has been realized in-house with a litz-wire winding on a coreless bobbin former, which results in very low losses. Its inductance measured was measured at the resonance frequency and it was found to be 7:4 nH. The two values of load resistances were selected for illustrating the results concerning the proposed control strategy, namely, $R = 54\ \Omega$ and $R = 48\ \Omega$. It is worth noting that with $R = 54\ \Omega$ ($Q \approx 2.1 > Q_{\text{sn}}$), a stable limit cycle exists but the system cannot converge to it under the conventional ZCS control and with zero ICs and that with $R = 48\ \Omega$ ($Q \approx 1.8 < Q_{\text{sn}}$), no stable limit cycle exists for the system under the conventional ZCS control [10], [11]. For its simplicity of implementation, the last technique based on hysteretic current feedback and edge-triggered flip-flop was used in the experimental tests. The waveforms of the output capacitor voltage v_C and the inductor current i_L are represented in Fig. 8. It can be observed that with both values of the load resistance, the proposed modification control strategy was capable to make the system to converge to the desired limit cycle with zero ICs. For $R = 54\ \Omega$, even after disabling the proposed control and switching to the conventional ZCS control strategy, the system continue working in the desired limit cycle because once the trajectory is inside its basin of attraction, the conventional ZCS control is enough to maintain the system operating with the same cycle. However, for $R = 48\ \Omega$, the system cannot continue working in the desired regime after switching to the conventional ZCS control strategy since no stable limit cycle exists in this case as explained previously. In this case, to reach a stable limit cycle, the modification on the ZCS control must be permanently enabled. By observing the current waveforms in the oscilloscope, it could be observed that between the zero current crossing instant and the effective switching instant, there is a total delay of about 118 ns. Note that except from the effect of this propagation delay, there is a good agreement

(a) $R = 54 \ \Omega$

(b) $R = 54 \ \Omega$

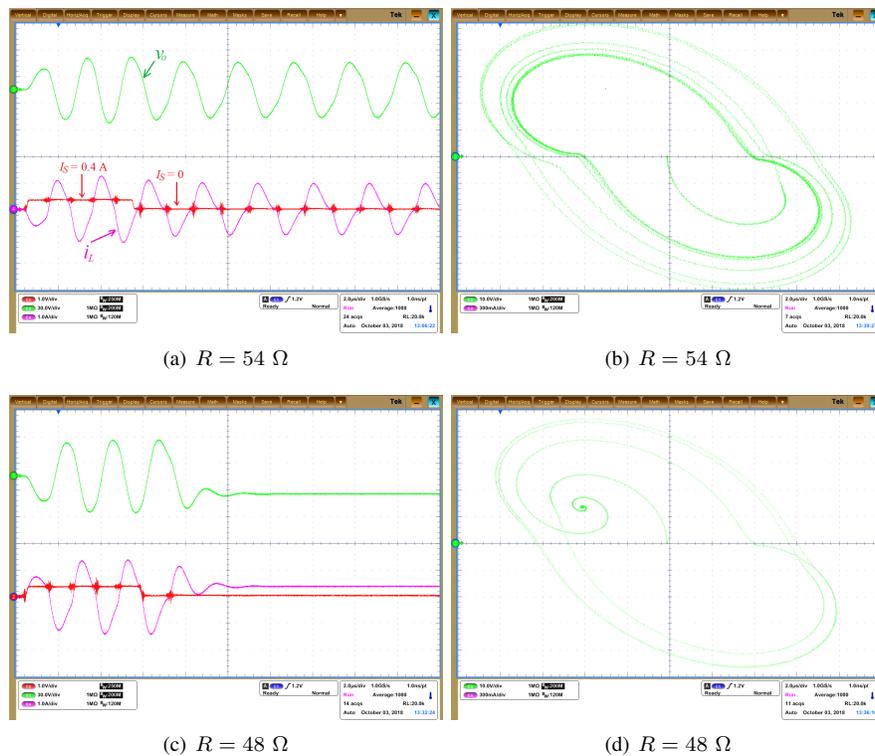(c) $R = 48 \ \Omega$

(d) $R = 48 \ \Omega$

Fig. 8. Experimental waveforms of the state variables and their corresponding state plane trajectories, by using the modified technique based on HCF. In both cases, this modification is disabled after 5 μs, then the system operates according to the conventional ZCS control.

between the real measurements in Fig. 8 and the corresponding simulated response.

VI. CONCLUSIONS

For relatively low values of the quality factor, the effect of the coexistence of attractors is prominent in parallel resonant converters and starting at the basin of attraction of the desired limit cycle is necessary for the system to reach this limit cycle. To protect the system from coexistence of other undesired attractors, four modified switching decisions that aims to make the the equilibrium points of the system virtual have been proposed. The first three proposed control techniques have all been proven to be useful to suppress undesired basin of attractions, thus facilitating the startup of the system from zero initial conditions. However, the forth proposed technique, that is the hysteretic current feedback (HCF), presents similar performances while being its implementation simple, thus requiring conventional low cost analog circuit devices. An experimental validation of this simple and low cost control technique has been provided.

REFERENCES

[1] S.-Y. Yu, R. Chen and A. Viswanathan, "Survey of Resonant Converter Topologies," 2018 *Texas Instruments*, Power Supply Design Seminar SEM2300, TI Literature Number: SLUP376, available at https://www.ti.com/seclit/ml/slup376/slup376.pdf
[3] R. Bonache-Samaniego, C. Olalla and L. Martinez-Salamero, "Design of self-oscillating resonant converters based on a variable structure systems approach," *IET Power Electronics,* vol. 57, no. 1, pp. 111-119, 2015.
[2] T. Qian, "A converter combination scheme for efficiency improvement of PV systems," *IEEE Trans. Circuits Syst. II, Exp. Briefs, early access,* 2017.
[4] R. Bonache-Samaniego, C. Olalla and L. Martinez-Salamero, "Dynamic Modeling and Control of Self-Oscillating Parallel Resonant Converters Based on a Variable Structure Systems Approach," *IEEE Transactions on Power Electronics,* vol. 32, no. 2, pp. 1469-1480, 2017.
[5] T. S. Chan and C. L. Chen, "A primary side control method for wireless energy transmission system," *IEEE Trans. Circuits Syst. I, Reg. Papers,* vol. 59, no. 8, pp. 1805-1814, 2012.
[6] R. Yang, H. Ding, Y. Xu, L. Yao, and Y. Xiang, "An analytical steady-state model of LCC type series-parallel resonant converter with capacitive output filter," *IEEE Trans. Power Electron.,* vol. 29, no. 1, pp. 328-338, 2014.
[7] J. Mućko and R. Strzelecki, "Errors in the analysis of series resonant inverter/converter assuming sinusoidal waveforms of voltage and current," 2016 10th International Conference on Compatibility, Power Electronics and Power Engineering (CPE-POWERENG), Bydgoszcz, 2016, pp. 369-374, 2016.
[8] S. Banerjee, "Coexisting attractors, chaotic saddles, and fractal basins in a power electronic circuit," *IEEE Transactions on Circuits and Systems I: Fundamental Theory and Applications,* vol. 44, no. 9, pp. 847-849, 1997.
[9] S. Seth and S. Banerjee, "Experimental Observation of Multiple Attractor Bifurcation in an Electronic Circuit," *IEEE Transactions on Circuits and Systems II: Express Briefs.*, doi: 10.1109/TCSII.2018.2828409.
[10] L. Benadero, E. Ponce, A. El Aroudi and L. Martinez-Salamero, "Analysis of coexisting solutions and control of their bifurcations in a parallel LC resonant inverter," 2017 *IEEE International Symposium on Circuits and Systems,* (ISCAS), Baltimore, MD, pp. 1-4, 2017.
[11] L. Benadero, E. Ponce, A. El Aroudi and F. Torres, "Limit cycle bifurcations in resonant LC power inverters under zero current switching strategy," *Nonlinear Dynamics,* vol. 91 no.2, pp. 1145-1161, 2018.
[12] A. El Aroudi, L. Benadero, E. Ponce, C. Olalla, F. Torres and L. Martinez-Salamero "Nonlinear Dynamic Modeling and Analysis of Self-Oscillating H-Bridge Parallel Resonant Converter Under Zero Current Switching Control: Unveiling Coexistence of Attractors," *IEEE Trans. CAS I,* submitted, 2018.